Available online at www.sciencedirect.com

ScienceDirect

Mendeleev Commun., 2021, **31**, 97–99

Mendeleev Communications

Hydroxyapatite of plate-like morphology obtained by low temperature hydrothermal synthesis

Victoria K. Besprozvannykh,[a] Ilya E. Nifant'ev,*[a,b] Alexander N. Tavtorkin,[a,b] Ivan S. Levin,[a] Andrey V. Shlyakhtin[a,b] and Pavel V. Ivchenko[a,b]

[a] *A. V. Topchiev Institute of Petrochemical Synthesis, Russian Academy of Sciences, 119991 Moscow, Russian Federation*

[b] *Department of Chemistry, M. V. Lomonosov Moscow State University, 119991 Moscow, Russian Federation. E-mail: inif@org.chem.msu.ru*

DOI: 10.1016/j.mencom.2021.01.030

The morphology of hydroxyapatite crystals formed in hydrothermal reaction of calcium EDTA complex with KH_2PO_4 at 120 °C depends on the pH value of the reaction medium. Bone-like platy microcrystals were prepared at pH 6, while at higher pH values rod-like species were obtained.

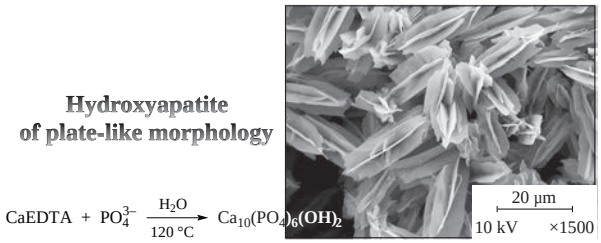

Keywords: calcium, crystallography, crystal morphology, EDTA, hydrothermal synthesis, hydroxyapatite, electron microscopy, X-ray diffraction.

Calcium hydroxyapatite $Ca_{10}(PO_4)_6(OH)_2$ (HAp) is the main inorganic part of mineralized tissues,[1–3] so synthetic HAp is regarded as a promising bone substituent.[4–14] In a natural bone tissue, HAp crystals constitute plates of nanosized thickness.[1,15,16] Material of similar platelet morphology was synthesized on the surface of HAp–tricalcium phosphate ceramics from hexagonal bipyramidal HAp single crystals and found to promote primary human osteoblast adhesion.[17] HAp platelets were shown to induce osteogenic differentiation of mesenchymal stem cells.[18] Hence, the preparation of the HAp nanosized plates to develop new composites for bone surgery and tissue engineering is a challenge in the materials science.

HAp crystallizes in a hexagonal crystal system with two major crystal planes. The *a* plane is enriched by Ca^{2+} ions and therefore is positively charged, the negatively charged *c* plane is enriched by phosphate and OH^- ions (Figure 1).[1,19] In bio-mineralized collagen fibrils, the HAp crystals expose predominantly their *a* planes, while the most of current laboratory methods allows one to obtain rod-like HAp crystals with the side *a*–*a* faces and the end *c* planes exposed or, alternatively, microspherical needle aggregates, mainly due to faster crystal growth along the *c* axis (see Figure 1).[20–26]

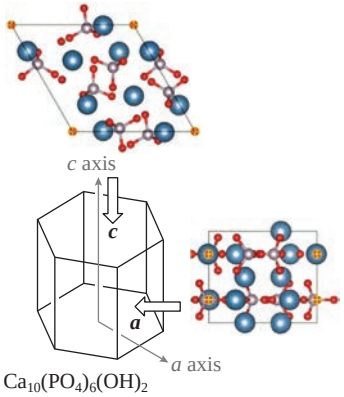

Figure 1 Crystal structure and crystal planes of HAp.

Our preliminary attempt to synthesize HAp employed a method closely related to the known one.[18] Starting from the aqueous solutions of $CaCl_2$ and Na_2HPO_4 at pH 9–10, we obtained two HAp samples with virtually identical rod-like morphology, X-ray diffraction (XRD) patterns and TEM images, despite the difference in the reaction temperature, namely 75 and 180 °C (for details, see Online Supplementary Materials).

The anisotropy of the HAp crystal planes allows one to suggest that the habit of the HAp crystals formed may be affected by composition of the reaction mixture. As it was previously demonstrated, the employment of the Ca^{2+} complexes with chelating carboxylic acids such as lactic,[27] citric,[28] or ethylenediaminetetraacetic acid (EDTA),[29–34] resulted in formation of the HAp crystals of various morphology, however the influence of reaction temperature and pH was not explored in depth.

Using the CaEDTA chelate complex as a Ca^{2+} source, we performed its reactions with KH_2PO_4 in aqueous media at different pH values and temperatures 100–120 °C.[†] The chelate complex employed is stable at room temperature even in a basic medium. On heating, the complex dissociates [reaction (1)] and

[†] $Ca(OH)_2$ (37.045 g, 0.5 mol) reacted with Na_2EDTA (186.12 g, 0.5 mol) in water (500 ml in total) resulting in 1 M solution of CaEDTA. This solution of CaEDTA (10 ml, 10 mmol), KH_2PO_4 (0.80 g, 5.9 mmol), water (30 ml) and calculated amount of NaOH (0 g for pH 6, 0.28 g for pH 9 or 0.50 g for pH 13) were placed into a 50 ml vessel. The vessel was closed by a rubber septum with an aluminum cap and heated at 120 °C for 2 h (the first series) or at 100 °C for 1 h and then at 120 °C for 1 h (the second series). The precipitate formed was washed with water (2 × 40 ml), then with EtOH (2 × 40 ml) and dried.

the Ca^{2+} ions formed react with phosphate resulting in HAp [reaction (2)].

$$CaEDTA \rightarrow Ca^{2+} + EDTA^{2-} \quad (1)$$

$$10\,Ca^{2+} + 6\,PO_4^{3-} + 2\,OH^- \rightarrow Ca_{10}(PO_4)_6(OH)_2\downarrow \quad (2)$$

In the first series of the hydrothermal synthesis using rapid heating to 120 °C and then reaction for 2 h at different pH values, HAp microcrystals with pH-dependent morphology were obtained. Under alkaline conditions (pH 13), cotton-like aggregates of needles having ~1 μm length and ~10 nm width were formed [Figure 2(*a*)]. At pH 9, the size of the needles was larger [Figure 2(*b*)] and at pH 6 the partial formation of plate-like crystals was detected [(Figure 2(*c*)]. XRD data of the crystaline phases (see Online Supplementary Materials) revealed, that at pH 6 the crystals were substantially formed by the growth along the *a* axis rather than *c* axis, contrary to the crystals obtained at higher pH values. Note that the morphology of the microcrystals synthesized at pH 6 [see Figure 2(*c*)] resembled the known habit of HAp crystals grown using hydrothermal synthesis at 200 °C and pH 11,[29] however the latter were clearly larger (Figure S6, see Online Supplementary Materials).

Unexpected and promising results were obtained in the second series of experiments, in which the reaction of CaEDTA with KH_2PO_4 was carried out in two stages, namely at 100 °C for 1 h and then at 120 °C for 1 h. At pH 13, dandelion-like HAp nanostructures were formed [Figure 2(*d*)]. At pH 9, the habit of microcrystals was different [Figure 2(*e*)] with preservation of crystal growth along the *c* axis (Figure 3). However, at pH 6, a substantial crystal growth along the *a* axis was detected from increased intensity of the (100) and (300) peaks [Figure 3(*c*)] with formation of microcrystals having unique platy morphology [Figure 2(*f*)].

Data on the XRD patterns for HAp samples obtained at different pH values are collected in Table 1 together with known data for the HAp films formed from plate-like and rod-like microcrystals.[18] It follows from Table 1 that the crystal structure of HAp synthesized at pH 6 is similar to that of platy HAp microcrystals with known enhanced osteogenic characteristics.[18]

In summary, by adjustment of pH for the hydrothermal synthesis, we obtained plate-like HAp species with promising morphology and crystal structure with potential application in the design of HAp-based composites for bone surgery.

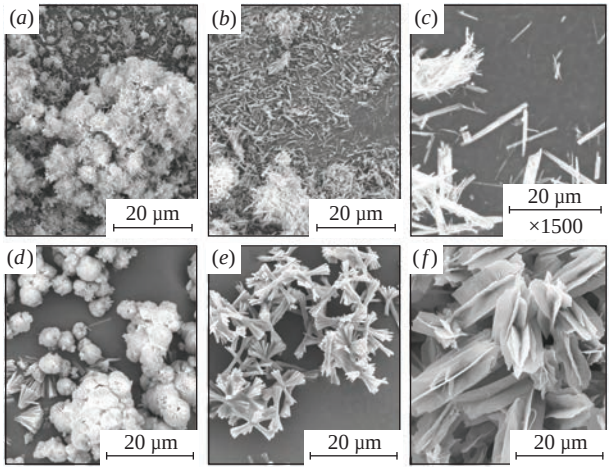

Figure 2 SEM images of HAp microcrystals obtained by mild hydrothermal synthesis: the first series at 120 °C for 2 h with pH values of (*a*) 13, (*b*) 9 and (*c*) 6 as well as the second series at 100 °C for 1 h then at 120 °C for 1 h with pH values of (*d*) 13, (*e*) 9 and (*f*) 6.

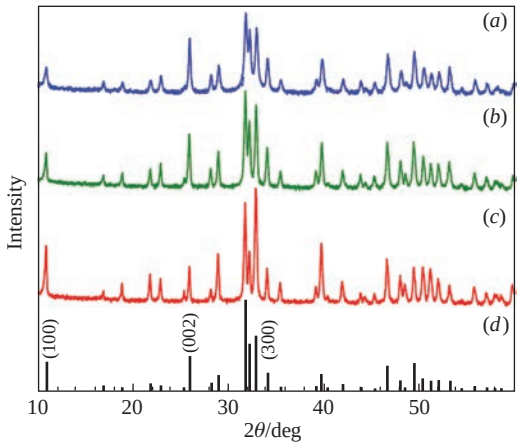

Figure 3 XRD patterns of HAp microcrystals obtained in the second series of the mild hydrothermal synthesis at pH (*a*) 13, (*b*) 9 and (*c*) 6, along with (*d*) reference HAp sample (JCPDS 09-0432).

Table 1 Morphology and ratio of characteristic XRD peaks for HAp crystals obtained by hydrothermal synthesis under various conditions.

Reaction temperature and time	pH	Crystal morphology	XRD (300) : (002) peaks intensity ratio
120 °C for 2 h (1st series)	6	plate-like	5.51
	9	rod-like	1.92
	13	rod-like	1.40
100 °C for 1 h, then 120 °C for 1 h (2nd series)	6	plate-like	5.42
	9	rod-like	1.95
	13	rod-like	1.83
ref. 18		plate-like	6.25
ref. 18		rod-like	1.25

This work was supported by the Russian Science Foundation (grant no. 16-13-10344) in the part of HAp synthesis and was carried out within the State Program of the A. V. Topchiev Institute of Petrochemical Synthesis, Russian Academy of Sciences, in the part of HAp analysis. Electron microscopy characterization was performed at the Division of Structural Studies of the N. D. Zelinsky Institute of Organic Chemistry, Russian Academy of Sciences.

Online Supplementary Materials

Supplementary data associated with this article can be found in the online version at doi: 10.1016/j.mencom.2021.01.030.

References

1 M. Okada and T. Matsumoto, *Jpn. Dent. Sci. Rev.*, 2015, **51**, 85.
2 L. C. Palmer, C. J. Newcomb, S. R. Kaltz, E. D. Spoerke and S. I. Stupp, *Chem. Rev.*, 2008, **108**, 4754.
3 N. Eliaz and N. Metoki, *Materials*, 2017, **10**, 334.
4 A. Haider, S. Haider, S. S. Han and I.-K. Kang, *RSC Adv.*, 2017, **7**, 7442.
5 Z. Bal, T. Kaito, F. Korkusuz and H. Yoshikawa, *Emergent Mater.*, 2020, **3**, 521.
6 H. A. Siddiqui, K. L. Pickering and M. R. Mucalo, *Materials*, 2018, **11**, 1813.
7 N. Ramesh, S. C. Moratti and G. J. Dias, *J. Biomed. Mater. Res., Part B*, 2018, **106**, 2046.
8 A. Kumar, S. Kargozar, F. Baino and S. S. Han, *Front. Mater.*, 2019, **6**, 313.
9 D. A. Florea, C. Chircov and A. M. Grumezescu, *Appl. Sci.*, 2020, **10**, 3483.
10 K. Zhang, Y. Zhou, C. Xiao, W. Zhao, H. Wu, J. Tang, Z. Li, S. Yu, X. Li, L. Min, Z. Yu, G. Wang, L. Wang, K. Zhang, X. Yang, X. Zhu, C. Tu and X. Zhang, *Sci. Adv.*, 2019, **5**, eaax6946.
11 G. Singh, R. P. Singh and S. S. Jolly, *J. Sol–Gel Sci. Technol.*, 2020, **94**, 505.
12 W. Habraken, P. Habibovic, M. Epple and M. Bohner, *Mater. Today*, 2016, **19**, 69.
13 J. Jeong, J. H. Kim, J. H. Shim, N. S. Hwang and C. Y. Heo, *Biomater. Res.*, 2019, **23**, 4.

14 J. Lu, H. Yu and C. Chen, *RSC Adv.*, 2018, **8**, 2015.
15 C. Burger, H.-w. Zhou, H. Wang, I. Sics, B. S. Hsiao, B. Chu, L. Graham and M. J. Glimcher, *Biophys. J.*, 2008, **95**, 1985.
16 B. Lowe, J. G. Hardy and L. J. Walsh, *ACS Omega*, 2020, **5**, 1.
17 G. Wang, Z. Lu, K. Y. Xie, W. Y. Lu, S. I. Roohani-Esfahani, A. Kondyurin and H. Zreiqat, *J. Mater. Chem.*, 2012, **22**, 19081.
18 C. Liu, H. Zhai, Z. Zhang, Y. Li, X. Xu and R. Tang, *ACS Appl. Mater. Interfaces*, 2016, **8**, 29997.
19 J. M. Hughes, M. Cameron and K. D. Crowley, *Am. Mineral.*, 1989, **74**, 870.
20 X. Ji, Z. Fang, X. Fan, J. Deng, R. Shan, Q. Li and C. Liu, *Mater. Lett.*, 2020, **271**, 127857.
21 M. Sadat-Shojai, M.-T. Khorasani, E. Dinpanah-Khoshdargi and A. Jamshidi, *Acta Biomater.*, 2013, **9**, 7591.
22 G. S. Han, S. Lee, D. W. Kim, D. H. Kim, J. H. Noh, J. H. Park, S. Roy, T. K. Ahn and H. S. Jung, *Cryst. Growth Des.*, 2013, **13**, 3414.
23 H. Zhou and J. Lee, *Acta Biomater.*, 2011, **7**, 2769.
24 A. Ezerskyte-Miseviciene and A. Kareiva, *Mendeleev Commun.*, 2019, **29**, 273.
25 V. Jonauske, R. Ramanauskas, R. Platakyte, G. Niaura, L. Mikoliunaite, K. Ishikawa and A. Kareiva, *Mendeleev Commun.*, 2020, **30**, 512.
26 I.-H. Lee, J.-A Lee, J.-H. Lee, Y.-W. Heo and J.-J. Kim, *J. Korean Ceram. Soc.*, 2020, **57**, 56.
27 R. K. Roeder, G. L. Converse, H. Leng and W. Yue, *J. Am. Ceram. Soc.*, 2006, **89**, 2096.
28 L. Pastero, M. Bruno and D. Aquilano, *Crystals*, 2018, **8**, 308.
29 M. Andrés-Vergés, C. Fernández-González and M. Martínez-Gallego, *J. Eur. Ceram. Soc.*, 1998, **18**, 1245.
30 A. Lak, M. Mazloumi, M. Mohajerani, A. Kajbafvala, S. Zanganeh, H. Arami and S. K. Sadrnezhaad, *J. Am. Ceram. Soc.*, 2008, **91**, 3292.
31 R. Zhu, R. Yu, J. Yao, D. Wang and J. Ke, *J. Alloys Compd.*, 2008, **457**, 555.
32 C. Yang, Z. Huan, X. Wang, C. Wu and J. Chang, *ACS Biomater. Sci. Eng.*, 2018, **4**, 608.
33 K. Suchanek, M. Perzanowski, J. Lekki, M. Strąg and M. Marszałek, *Ceramics*, 2019, **2**, 180.
34 R. Chen and J. Shen, *Mater. Lett.*, 2020, **259**, 126881.

Received: 5th October 2020; Com. 20/6328